GDCh

Communications

Angewandte
Chemie
International Edition
www.angewandte.org

VIP **Host-Guest Chemistry** *Very Important Paper*

Guest-Dependent Isomer Convergence of a Permanently Fluxional Coordination Cage

André P. Birvé, Harshal D. Patel, Jason R. Price, Witold M. Bloch,* and Thomas Fallon*

Abstract: *A fluxional bis-monodentate ligand, based on the archetypal shape-shifting molecule bullvalene, self-assembles with M^{2+} ($M = Pd^{2+}$ or Pt^{2+}) to produce a highly complex ensemble of permanently fluxional coordination cages. Metal-mediated self-assembly selects for an M_2L_4 architecture while maintaining shape-shifting ligand complexity. A second level of simplification is achieved with guest-exchange; the binding of halides within the M_2L_4 cage mixture results in a convergence to a cage species with all four ligands present as the "B isomer". Within this confine, the reaction graph of the bullvalene is greatly restricted, but gives rise to a mixture of 38 possible diastereoisomers in rapid exchange. X-ray crystallography reveals a preference for an achiral form consisting of both ligand enantiomers. Through a combination of NMR spectroscopy and DFT calculations, we elucidate the restricted isomerisation pathway of the permanently fluxional M_2L_4 assembly.*

Through unending sequences of sigmatropic rearrangements, *bullvalene* exists as an ensemble of >1.2 million degenerate isomers and has no permanent carbon–carbon bonds.[1] The introduction of substituents gives rise to ensembles of non-degenerate isomers, whereby substituents may adopt all possible structural relationships. While the chemistry of this remarkable hydrocarbon dates back to the 1960s,[2] its development was slowed by arduous synthetic access. A recent revival of interest has been led by Bode,[3] Echavarren,[4] and one of our laboratories.[5] In a recent report, we developed easy synthetic access to a range of diaryl substituted bullvalenes.[5c]

The coordination chemistry of bullvalene as a shape-shifting ligand is completely unexplored, save for a few early reports of metal–diene complexation to the parent hydrocarbon.[6] Bidentate substituted bullvalenes as ligands offer the potential to impart dynamic host-guest binding. Pioneering studies by Bode have demonstrated both fullerene and polyol host-guest binding to multi-functionalised bullvalenes in highly complex, though structurally ill-defined, settings.[3b–c,g]

In conceptualising bis-pyridyl bullvalene as a bis-monodentate ligand, a range of N–N bite angles are possible through interconversion of its major isomers (Figure 1). Given this geometric variability, metal coordination by fluxional ligands has the potential to produce highly complex and dynamic mixtures. Considering this, we prepared a 3-substituted bis-pyridyl bullvalene to examine its coordination chemistry in the structurally well-defined setting of M_2L_4 coordination cages (Figure 1).

M_2L_4 coordination cages are accessible metallo-supramolecular hosts, typically assembled from concave-shaped ditopic ligands and square planar metal centres.[7] Their simple and symmetrical structure has served as a platform to introduce various stimuli responsive properties[8] and control self-sorting phenomena through ligand design.[9] Most of these advances have been achieved with symmetrical and static ligands that produce only single cage isomers upon complexation with metal ions.[9b] On the other hand, utilising unsymmetrical ligands[10] or ligands with rotational isomerism[11] results in isomeric cage mixtures that require steric or geometric constraints to achieve defined structures. In this context, coordination cages composed of permanently fluxional, shape-shifting ligands are hitherto unexplored.

Herein we present the self-assembly and guest-induced isomer amplification of an M_2L_4 coordination cage assembled from bis-3-pyridyl bullvalene. Whilst a highly complex isomeric mixture is obtained in the presence of
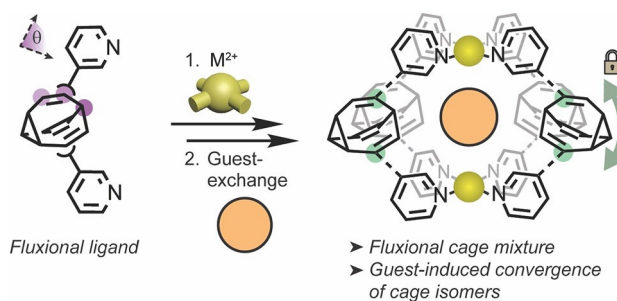
[*] A. P. Birvé, H. D. Patel, W. M. Bloch, T. Fallon
Department of Chemistry, University of Adelaide
Adelaide 5005 (Australia)
E-mail: witold.bloch@adelaide.edu.au
        thomas.fallon@adelaide.edu.au

Dr. J. R. Price
ANSTO, Australian Synchrotron,
800 Blackburn Road, Clayton, Vic 3168 (Australia)

Figure 1. Metal-mediated self-assembly of bis-3-pyridyl bullvalene forms a complex mixture of fluxional M_2L_4 cage isomers. Guest exchange restricts the fluxional behaviour of the assembly resulting in a significant convergence to an "all-B" isomer form.

BF_4^- counterions, the presence of a suitable guest results in a significant convergence to a defined M_2L_4 cage isomer that remains permanently fluxional through a restricted pathway. Through a combination of NMR spectroscopy, X-ray crystallography, and DFT calculations, we map out the fluxional pathway of the bullvalene derived ligand within the confines of the M_2L_4 assembly.

Our study commenced with the synthesis of bis-3-pyridyl bullvalene via a Suzuki coupling between bis-(Bpin) bullvalene and 3-bromopyridine in excellent yield (Figure 2a). Variable temperature (VT) ^1H NMR spectroscopy in CD_3CN revealed that the ligand exists in a dynamic equilibrium between three major isomers: A, B, and C in a 48:38:13 ratio respectively, in rapid exchange at room temperature (Figure S1).

Treatment of the ligand with 0.5 equivalents of [Pd-$(CH_3CN)_4](BF_4)_2$ initially led to an intractable complex mixture denoted **1·BF₄** (Figure 2b). The broad signals observed in the room temperature ^1H NMR spectrum resolved somewhat at $-35°C$, and the NCH pyridyl resonances were observed downfield relative to the free ligand indicating coordination to Pd^{2+} (Figure 2b, Figure S1). The anticipated Pd_2L_4 structure was confirmed by ESI-HRMS, with evident peaks of the cage at 479, 762, and 1611 m/z corresponding to $[Pd_2L_4 + n\,BF4]^{4-n}$ ($n = 1–3$) (Figure 2b, Figure S8). Consistent with the complex mixture, the

^{19}F NMR spectrum of **1·BF₄** revealed a multitude of resonances corresponding to various isomers encapsulating BF_4^- (Figure S7).

The addition of one equivalent of chloride to **1·BF₄** resulted in complete exchange of the encapsulated anion, producing a significantly resolved ^1H NMR spectrum containing one dominant cage species, **1·Cl** (Figure 2c). Anion exchange of **1·BF₄** or **1·Cl** with an equivalent of iodide produced the corresponding Pd_2L_4 cage **1·I** (Figure 2d).[12] ^1H NMR analysis of **1·Cl** and **1·I** at $-35°C$ revealed the dominance of *isomer B* of the ligand in solution, indicating a complete change in the isomer distribution of the bullvalene relative to the parent complex **1·BF₄**. However, the dynamic nature of the bullvalene ligand core persists as shown by characteristically broad signals in the room temperature ^1H NMR spectra (Figure S19). ESI-HRMS was indicative of a Pd_2L_4 structure in each case, with prominent $[Pd_2L_4 + X + n\,BF4]^{3-n}$ ($X = Cl^-$ or I^-, $n = 0–1$) peaks supporting the encapsulation of the respective anion within the central cavity of the cage.

Several other Pd_2L_4 cages were prepared via anion exchange with **1·BF₄**, in order to compare binding preferences of the system. Larger counterions such as PF_6^- do not undergo anion exchange with the M_2L_4 assembly, leading to complex spectra analogous to that in Figure 2b (see Supporting Information for full details). Anion exchange with NO_3^- on the other hand, produced a ^1H NMR spectrum with the isomer B ligand predominating amongst other unresolvable species (Figure S9). Across the anionic guests that were investigated, only halides resolved the fluxional mixture to a dominant *isomer B* cage species, with preferential binding observed for larger halides (e.g. I^- over Cl^-). Analysis of the HRMS spectra of these samples confirmed the Pd_2L_4 structure and the absence of higher nuclearity M_nL_{2n} species (see Supporting Information for full details) that could be afforded by other isomers of bis-3-pyridyl bullvalene.

We also prepared the Pt_2L_4 analogues of the BF_4^-, Cl^-, and I^- encapsulated cages (denoted as **1′·BF₄**, **1′·Cl**, and **1′·I**); heating at $85°C$ was required to induce anion exchange for the Pt_2L_4 cages indicating a dissociative exchange mechanism. Each of these cages displays near identical characteristics to their corresponding palladium cage by VT NMR spectroscopy. Together, these results indicate that the fluxional behaviour of the ligand within the M_2L_4 structure occurs without metal-ligand dissociation as a requirement. ^1H EXSY NMR measurements on **1·I** revealed the exchange of particular bullvalene proton signals, indicative of isomer B to B′ isomerism with a rate constant of $\approx 0.7\,s^{-1}$ at $-20°C$ (see Supporting Information for full details). This establishes the mode of isomerism within the cage, and this rate constant is broadly consistent with the calculated barrier of ligand isomerisation (see below).

The conceivable complexity of this M_2L_4 system is built upon the reaction graph of the bullvalene ligand. For disubstituted bullvalene networks of this type, there are 15 possible isomers including three enantiomer pairs, (Figure 3b) where nodes represent isomers and edges Cope rearrangement pathways.[5c] For bis-3-pyridyl bullvalene
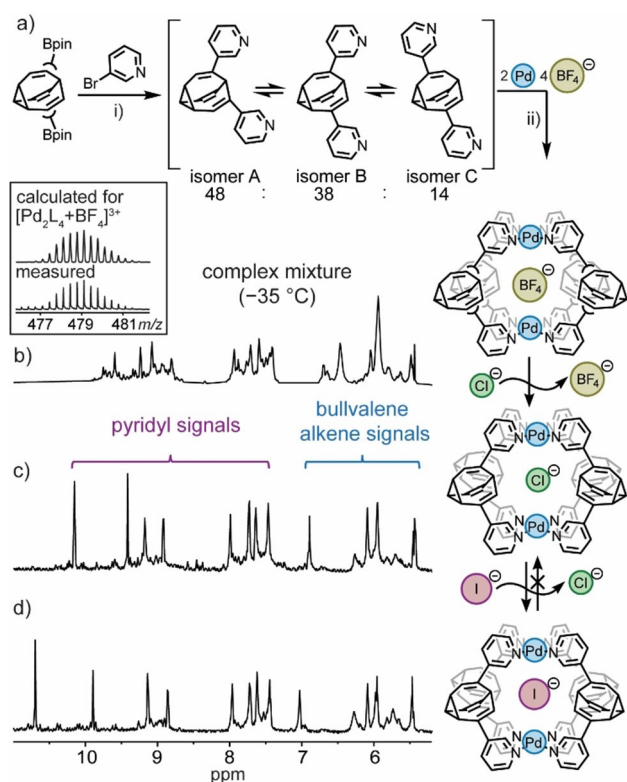

Figure 2. a) Synthesis of bis-3-pyridyl bullvalene, Pd_2L_4 cage assembly, guest exchange, and NMR analysis. i) Pd(PPh₃)₄ 5 mol%, NaOH, THF/H₂O, 65°C, 92%; ii) [Pd(CH₃CN)₄](BF₄)₂, 0.5 equiv, CD₃CN, 60°C, 10 min. ^1H NMR spectra ($-35°C$, CD₃CN) of b) **1·BF₄** (ESI-HRMS shown in inset); c) **1·Cl**; d) **1·I**.

Angew. Chem. Int. Ed. **2022**, *61*, e202115468 (2 of 5)

© 2021 The Authors. Angewandte Chemie International Edition published by Wiley-VCH GmbH
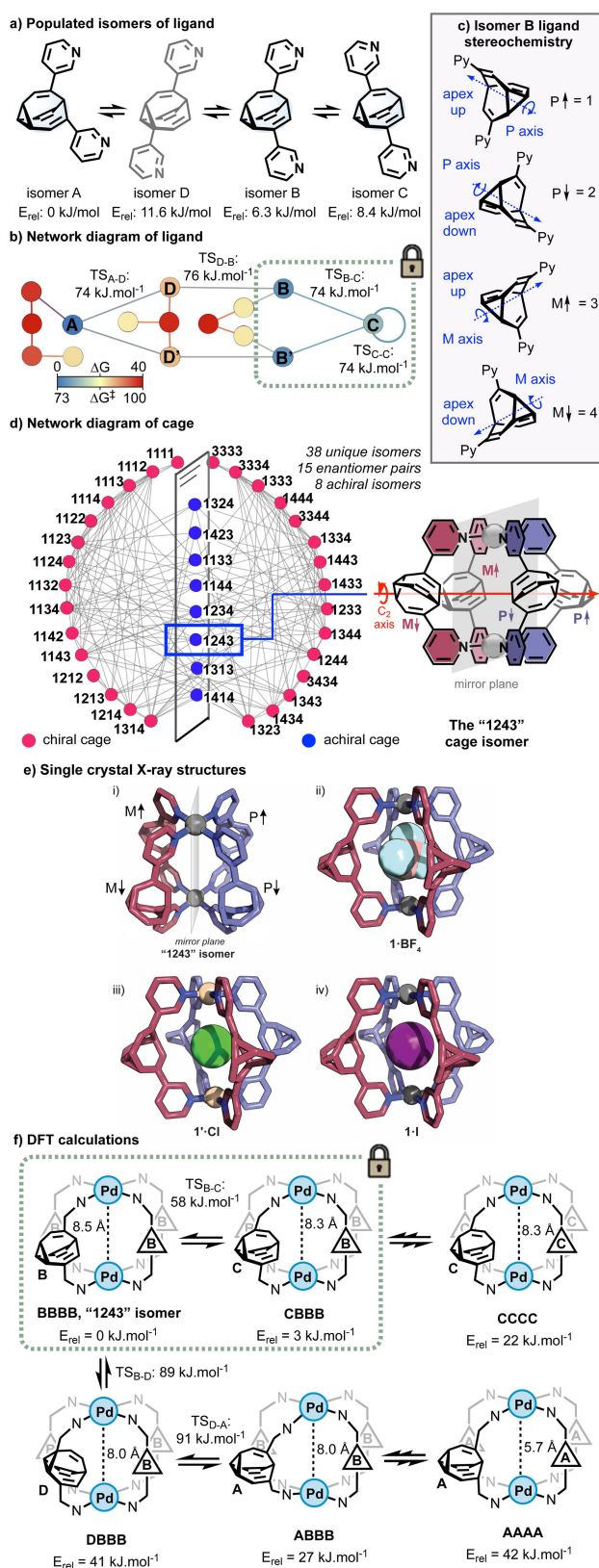
Figure 3. a) Isomer distribution of the ligand. b) Ligand reaction graph. c) Stereoisomerism of isomer B. d) Network diagram of the all-B M_2L_4 cage. e) X-ray structures of "1243" bullvalene cage isomer i) A perspective view of **1** highlighting the symmetry elements and directionality of the cyclopropane ring in each bullvalene ligand enantiomer ; ii) **1·BF₄**; iii) **1′·Cl**; iv) **1·I**. f) DFT analysis of Pd_2L_4 cages.

there are three populated isomers, A, B, and C, that rapidly interconvert through a lower energy circuit including intermediate isomer D. Isomer C also possesses a degenerate rearrangement pathway with itself (Figure 3b). DFT calculations provide a predicted energy dimension to this reaction graph (colour coded in Figure 3b, see Supporting Information for full details).

In combining four bullvalene ligands into an M_2L_4 cage, the potential level of complexity is enormous. If all possible bullvalene isomers could combine in all possible permutations, there would be approximately two hundred thousand possible isomeric cages.[13] However, all experimental evidence indicates isomer B as the predominant ligand isomer within the cage. This isomer is axially chiral, and its *Plus/Minus* (*P/M*) descriptors are defined by considering an axis that runs from the centre point of the cyclopropane through the apical bridgehead (or apex) of bullvalene.[5d] Within the cage, isomer B also possesses a vertical *directionality* relative to an arbitrary top-view of the cage, which we define as the *up/down* tilt of the apex. Thus, each coordinated ligand possesses two independent stereochemical degrees of freedom that may dynamically interconvert. This gives four possible ligands that make up the "all-B" cage which we label 1 (*P↑*), 2 (*P↓*), 3 (*M↑*), and 4 (*M↓*) (Figure 3c). A reaction graph of all possible all-B cages is shown in Figure 3d. From this we have an isomer list with 38 possible all-B cages, including 15 enantiomer pairs (red) and 8 achiral cages (blue). Each all-B isomer cage may interconvert with every other, as represented by the graph edges.

The isomerism, directionality, and chirality of the bullvalene ligand within the M_2L_4 cage was determined by single-crystal X-ray analysis. Single crystals of **1·BF₄**, **1·NO₃**, **1·I**, and **1′·Cl** were obtained by slow vapour diffusion of diisopropyl ether into CD_3CN solutions of the respective samples. All four samples crystallise in the monoclinic space group *C2/m*, and the contents of the asymmetric unit for each complex comprises of two crystallographically unique B ligand isomers (*M* and *P* enantiomers) coordinating to a metal centre of a separate M_2L_4 cage.[14] The remaining ligands from each identical but crystallographically independent cage molecule are generated by a horizontal mirror plane and C_2 axis of symmetry. The crystallised M_2L_4 isomer for each sample is composed of an all-B *cis*-configuration of *P* and *M* bullvalene enantiomers, giving a "1243" or *P↑-P↓-M↓-M↑* configuration (Figure 3e). Across the three Pd_2L_4 structures, the average Pd···Pd distance is 8.49 ± 0.07 Å, whilst the Pt_2L_4 assembly has a slightly shorter metal separation of 8.40 Å. In all structures the respective anion was located inside the central cavity of the cage.

While the exclusive preference for the 1243 B isomer (across a multitude of counterions) in the crystal lattice cannot be explained energetically, it is rational. This isomer represents the maximum degree of entropy, with respect to its stereochemical degrees of freedom, as well as maximum symmetry, bearing both an internal mirror plane and a C_2 axis.[15]

To understand the cage isomer convergence in the presence of halide guests, we undertook *VOIDOO* calculations on the X-ray structures of **1**. Based on a 1.4 Å probe,

a cavity volume of 69.7 Å³ was obtained for **1**. For BF_4^-, NO_3^-, I^-, and Cl^- as the counterions, the packing coefficients are 76%, 59%, 50%, and 34% respectively (Supporting Information, Table S5). As the decreasing packing coefficient correlates well to the experimental convergence of M_2L_4 isomers in solution, we postulate that optimal host–guest interactions, particularly for smaller spherical guests, drive the cage isomer convergence.[11a,16]

Together, these results show that the guest-driven convergence of the M_2L_4 system significantly simplifies the reaction graph of bullvalene, constraining it to a dominant B-isomer form. To further rationalise the structural preferences and dynamic behaviour of the Pd_2L_4 cages, we turned to computational modelling. Geometry optimisations were performed for a series of cage isomers at the B3LYP/Def2-SVP level on the respective tetracations in the gas phase. While this computational methodology doesn't carry the expectation of reliable chemical accuracy, the qualitative relative energies and geometry constraints are indicative.

Six structures were considered as exemplars of the AAAA, BBBA, BBBB, BBBC, BBBD, and CCCC cage isomers (Figure 3f). The BBBB "1243" isomer was found to be the lowest energy of the structures considered with a Pd–Pd distance of 8.46 Å (in excellent agreement with the crystal structure's average Pd–Pd distance of 8.49 Å). Isomerisation of one of the B ligands to its corresponding C ligand gives the BBBC cage which is only 3 kJ mol⁻¹ elevated in energy and nearly identical in its geometric parameters (Pd–Pd distance 8.3 Å). Further isomerisation to the CCCC cage gives a structure with similar overall geometry and somewhat elevated energy. Conversion of the ligand from the B isomer to the A isomer is more problematic. Firstly, the B isomer must transit isomer D, whereby the BBBD cage incurs a small contraction of the Pd–Pd distance to 8.0 Å and a moderate energy increase. From there, the D isomer must transit to isomer A giving the intermediate BBBA cage.

While the Pd–Pd distance of this cage is the same as that of BBBD, the energy is significantly elevated and there is a pronounced distortion of the regular M_2L_4 geometry whereby the planes of the square planar coordination around palladium are tilted by 12° with respect to one another (see Supporting Information for full details). Further isomerisation to the AAAA cage gives a structure that is elevated in energy by 46 kJ mol⁻¹ and has a short Pd–Pd distance of 5.7 Å (Figure 3f). Such a cage would have an internal cavity too small to encapsulate common anions (27.4 Å³ as indicated by VOIDOO calculations), and would have a significantly shorter metal–metal distance than any M_2L_4 cage reported in the literature (the shortest appears to be 6.5 Å reported by Puddephatt).[17]

From this we may rationalise the preponderance of ligand isomer B in M_2L_4 cages, their rapid interconversion through a B-C-B′ pathway, and the exclusion of isomer A from the reaction graph of the cage. Within the cage, each ligand may be considered as geometrically "pinned", with its pyridyl nitrogen–nitrogen distances fixed in place. This excludes transition to the more contracted A isomer, and that region of the reaction graph is shut down. However,

rapid B-B′ isomerism is still possible via isomer C, leading to dynamic diastereoisomer ensembles of "all-B" M_2L_4 cages. While Bode[3] has previously demonstrated abstract shifts in bullvalene isomer distributions through host–guest chemistry, this is the first time whereby imposed changes on the reaction graph of a bullvalene have been structurally mapped.

In summary, we have reported and structurally characterised the first permanently fluxional coordination complex of bullvalene. Self-assembly of bis-3-pyridyl bullvalene with Pd^{2+} or Pt^{2+} metal ions in the presence of BF_4^- counterions produced a complex M_2L_4 coordination cage mixture. Anion exchange with smaller anionic guests (e.g. Cl^- and I^-) led to a dramatic convergence to a well-defined all-B isomer cage complex; in solution this isomeric form remains fluxional, even within the kinetically inert Pt_2L_4 cage scaffold. X-ray crystallography revealed that the all-B cage is selective for the "1243" isomer. EXSY data and computational methods revealed that the all-B isomer host-guest complex undergoes a restricted B-C-B′ isomerisation, thus removing a huge fraction of complexity by shutting down other potential isomerisation circuits. We hope this work will inform the design of dynamic metallo-supramolecular systems that can undergo stimuli-responsive shape and size adaptability.

Conflict of Interest

The authors declare no conflict of interest.

Data Availability Statement

The data that support the findings of this study are available in the Supporting Information of this article.

[1] W. von E. Doering, W. R. Roth, *Tetrahedron* **1963**, *19*, 715–737.

[2] a) G. Schröder, *Angew. Chem.* **1963**, *75*, 722; b) R. Merényi, J. F. M. Oth, G. Schröder, *Chem. Ber.* **1964**, *97*, 3150–61; c) G. Schröder, R. Merényi, J. F. M. Oth, *Tetrahedron Lett.* **1964**, *5*, 773–777; d) G. Schröder, *Chem. Ber.* **1964**, *97*, 3140–9;

e) J. F. M. Oth, R. Merényi, J. Nielsen, G. Schröder, *Chem. Ber.* **1965**, *98*, 3385–400. For recent reviews see: f) S. Ferrer, A. M. Echavarren, *Synthesis* **2019**, *51*, 1037–1048; g) A. N. Bismillah, B. M. Chapin, B. A. Hussein, P. R. McGonigal, *Chem. Sci.* **2020**, *11*, 324–332.

[3] a) A. R. Lippert, J. Kaeobamrung, J. W. Bode, *J. Am. Chem. Soc.* **2006**, *128*, 14738–14739; b) A. R. Lippert, V. L. Keleshian, J. W. Bode, *Org. Biomol. Chem.* **2009**, *7*, 1529–1532; c) A. R. Lippert, A. Naganawa, V. L. Keleshian, J. W. Bode, *J. Am. Chem. Soc.* **2010**, *132*, 15790–15799; d) M. He, J. W. Bode, *Proc. Natl. Acad. Sci. USA* **2011**, *108*, 14752–14756; e) K. K. Larson, M. He, J. F. Teichert, A. Naganawa, J. W. Bode, *Chem. Sci.* **2012**, *3*, 1825–1828; f) M. He, J. W. Bode, *Org. Biomol. Chem.* **2013**, *11*, 1306–1317; g) J. F. Teichert, D. Mazunin, J. W. Bode, *J. Am. Chem. Soc.* **2013**, *135*, 11314–11321.

[4] a) S. Ferrer, A. M. Echavarren, *Angew. Chem. Int. Ed.* **2016**, *55*, 11178–11182; *Angew. Chem.* **2016**, *128*, 11344–11348; b) P. R. McGonigal, C. de León, Y. Wang, A. Homs, C. R. Solorio-Alvarado, A. M. Echavarren, *Angew. Chem. Int. Ed.* **2012**, *51*, 13093–13096; *Angew. Chem.* **2012**, *124*, 13270–13273.

[5] a) O. Yahiaoui, L. F. Pašteka, B. Judeel, T. Fallon, *Angew. Chem. Int. Ed.* **2018**, *57*, 2570–2574; *Angew. Chem.* **2018**, *130*, 2600–2604; b) O. Yahiaoui, L. F. Pašteka, C. J. Blake, C. G. Newton, T. Fallon, *Org. Lett.* **2019**, *21*, 9574–9578; c) H. D. Patel, T.-H. Tran, C. J. Sumby, L. F. Pašteka, T. Fallon, *J. Am. Chem. Soc.* **2020**, *142*, 3680–3685; d) O. Yahiaoui, H. D. Patel, K. S. Chinner, L. F. Pašteka, T. Fallon, *Org. Lett.* **2021**, *23*, 1157–1162.

[6] a) M. G. Newton, I. C. Paul, *J. Am. Chem. Soc.* **1966**, *88*, 3161–3162; b) J. S. McKechnie, M. Gary Newton, I. C. Paul, *J. Am. Chem. Soc.* **1967**, *89*, 4819–4825; c) R. Aumann, *Angew. Chem. Int. Ed. Engl.* **1970**, *9*, 800–801; *Angew. Chem.* **1970**, *82*, 810–811.

[7] a) M. Han, D. M. Engelhard, G. H. Clever, *Chem. Soc. Rev.* **2014**, *43*, 1848–1860; b) T. R. Cook, P. J. Stang, *Chem. Rev.* **2015**, *115*, 7001–7045; c) M. M. J. Smulders, I. A. Riddell, C. Browne, J. R. Nitschke, *Chem. Soc. Rev.* **2013**, *42*, 1728–1754.

[8] a) J. E. M. Lewis, E. L. Gavey, S. A. Cameron, J. D. Crowley, *Chem. Sci.* **2012**, *3*, 778–784; b) R.-J. Li, J. Tessarolo, H. Lee, G. H. Clever, *J. Am. Chem. Soc.* **2021**, *143*, 3865–3873; c) D. Yang, L. K. S. von Krbek, L. Yu, T. K. Ronson, J. D. Thoburn, J. P. Carpenter, J. L. Greenfield, D. J. Howe, B. Wu, J. R. Nitschke, *Angew. Chem. Int. Ed.* **2021**, *60*, 4485–4490; *Angew. Chem.* **2021**, *133*, 4535–4540; d) Z. Yang, J.-M. Lehn, *J. Am. Chem. Soc.* **2020**, *142*, 15137–15145; e) W. Wang, Y.-X. Wang, H.-B. Yang, *Chem. Soc. Rev.* **2016**, *45*, 2656–2693; f) A. J. McConnell, C. S. Wood, P. P. Neelakandan, J. R. Nitschke, *Chem. Rev.* **2015**, *115*, 7729–7793.

[9] a) W. M. Bloch, G. H. Clever, *Chem. Commun.* **2017**, *53*, 8506–8516; b) S. Pullen, J. Tessarolo, G. H. Clever, *Chem. Sci.* **2021**, *12*, 7269–7293.

[10] a) D. Ogata, J. Yuasa, *Angew. Chem. Int. Ed.* **2019**, *58*, 18424–18428; *Angew. Chem.* **2019**, *131*, 18595–18599; b) J. E. M. Lewis, J. D. Crowley, *ChemPlusChem* **2020**, *85*, 815–827; c) J. E. M. Lewis, A. Tarzia, A. J. P. White, K. E. Jelfs, *Chem. Sci.* **2020**, *11*, 677–683.

[11] a) T. Tsutsui, L. Catti, K. Yoza, M. Yoshizawa, *Chem. Sci.* **2020**, *11*, 8145–8150; b) A. W. Markwell-Heys, M. L. Schneider, J. Marie, L. Madridejos, G. F. Metha, W. M. Bloch, *Chem. Commun.* **2021**, *57*, 2915–2918.

[12] We've shown that anion exchange can be reversed on treatment of the **1·I** solution with one equivalent of AgBF$_4$.

[13] This modest overestimate is based on considering the chiral isomers, each with two stereochemical degrees of freedom within the cage and nine achiral isomers with one degree of freedom, giving 30 possible nonidentical ligands within the cage. The total number of cage isomers would be $30^4/4 = 202500$, not counting degeneracies associated with internal symmetry elements within some cages.

[14] Deposition Numbers 2105772, 2105771, 2120298, and 2120297 contain the supplementary crystallographic data for this paper. These data are provided free of charge by the joint Cambridge Crystallographic Data Centre and Fachinformationszentrum Karlsruhe Access Structures service www.ccdc.cam.ac.uk/structures.

[15] As **1·BF$_4$** and **1·NO$_3$** exist as mixtures of M$_2$L$_4$ assemblies in solution, we cannot rule out the influence of crystal-packing effects on the convergence to this single isomer in the solid-state.[5c, 11b] For a recent report on shape selective crystallisation, see: A. N. Bismillah, J. Sturala, B. M. Chapin, D. S. Yufit, P. Hodgkinson, P. R. McGonigal, *Chem. Sci.* **2018**, *9*, 8631–8636.

[16] S. Mecozzi, J. Rebek Julius, *Chem. Eur. J.* **1998**, *4*, 1016–1022.

[17] N. L. S. Yue, D. J. Eisler, M. C. Jennings, R. J. Puddephatt, *Inorg. Chem. Commun.* **2005**, *8*, 31–33.

[18] N. P. Cowieson, D. Aragao, M. Clift, D. J. Ericsson, C. Gee, S. J. Harrop, N. Mudie, S. Panjikar, J. R. Price, A. Riboldi-Tunnicliffe, R. Williamson, T. Caradoc-Davies, *J. Synchrotron Radiat.* **2015**, *22*, 187–190.

[19] D. Aragão, J. Aishima, H. Cherukuvada, R. Clarken, M. Clift, N. P. Cowieson, D. J. Ericsson, C. L. Gee, S. Macedo, N. Mudie, S. Panjikar, J. R. Price, A. Riboldi-Tunnicliffe, R. Rostan, R. Williamson, T. T. Caradoc-Davies, *J. Synchrotron Radiat.* **2018**, *25*, 885–891.